Spring 5-9-2020

# Delaying Flow Separation Using Piezoelectric Actuators

Kenechukwu Okoye

# Delaying Flow Separation Using Piezoelectric Actuators

by

**Kenechukwu Okoye**

A thesis submitted to the faculty of The University of Mississippi in partial fulfillment of the requirements of the Sally McDonnell Barksdale Honors College.

Oxford

April 2020

Approved By

Advisor: Dr Taiho Yeom

Reader: Dr Wen Wu

Reader: Dr Tejas Pandya

# DEDICATION

I dedicate this study to the Almighty God. Thank you for this opportunity you created for me, for your guidance and strength to complete this work. Thank you for the success of this study.

I'd also like to dedicate this study to my parents, Sir and Lady Okoye, who served as my role models, who encouraged me to never stop believing in myself the same way they never stopped believing in me.

Finally, I'd like to dedicate this study to the rest of my family and my friends for their continued support and love. Special thanks to Dami, you always made sure I never doubted that I could do this.

# ACKNOWLEDGEMENTS

I'm grateful to my research advisor, Dr Taiho Yeom, a Mechanical Engineering Professor at the University of Mississippi, who brought me into the research team and guided me through the study. He always gave good advice whenever I needed help with the research topics.

I'd also like to acknowledge Mukesh Ghimire, a fellow member of the research team who designed and fabricated the oval loop structure for the piezoelectric actuator and whose work was instrumental in the completion of this study.

Finally, I'll like to thank the Machine Shop Supervisor of the Mechanical Engineering Department at the University of Mississippi, Mr Matt Lowe, who taught me a lot about the practical aspects of engineering and provided invaluable assistance through out the course of the study.

# ABSTRACT

Flow separation causes aircraft to experience an increase in drag degrading their aviation performance. The goal of the study was to delay flow separation on an airfoil by embedding a high-frequency translational piezoelectric actuator along the surface of the airfoil. This study investigated the extent to which the high-frequency translational piezoelectric actuator displaces the flow separation downstream or prevents it altogether utilizing a fog-based flow visualization experiment. The actuators with two actuation surfaces were embedded on the suction surface of an Eppler 862 airfoil model and placed in a low-speed wind tunnel. Dry ice fog streams were injected into the wind tunnel and illuminated by a continuous laser in order to visualize the flow. Consecutive pictures of the flow field around the airfoil were taken every 5 microseconds using a high speed camera in order to observe the flow separation phenomenon before and after turning on the high-frequency translational surface actuation. The effects of the actuation on the flow separation were observed at different surface displacements ranging up to 0.12 mm at a 565 Hz operating frequency, angles of attack ranging up to $24^o$, and wind tunnel free stream velocities increased up to 12.7 m/s. As a result, the flow visualization study confirmed that the employed high-frequency translational surface actuation had the obvious control authority on delaying or suppressing the flow separation over the airfoil depending on the parameters changed.

# Contents

# List of Tables

# List of Figures

# Introduction

The adverse pressure gradient around airfoils gets stronger as the angle of attack becomes steeper. This makes the boundary layer slower and in some cases causes it to have zero velocity or to reverse in direction. This causes it to be forced away from the airfoil surface; this phenomenon is called Flow Separation. As the angle of attack increases, and the flow separation increases, there is an increase in pressure drag. If severe enough this could cause stalling. The increased pressure drag and stall are generally undesired outcomes in an aircraft because they cause an aircraft to be less efficient. Therefore, a lot of effort has been put into delaying flow separation in order to improve the efficiency of aircraft. Boundary layer control is any process which causes a boundary layer to behave differently than it normally would when it is developing naturally along a smooth surface [1].

The German engineer Ludwig Prandtl pioneered the use of flow control as it is seen today. He developed the boundary layer theory and described several experiments in which the boundary layer was controlled [2]. The general approach in controlling flow separation is to add momentum to the region of flow very close to the wall. This can be done by passive flow control i.e transferring momentum from regions farther from the wall. This could also be accomplished by active flow control i.e adding momentum from a propulsive system. Active flow control

tends to be more popular because passive flow control cannot be turned off when flow control is not required and this tends to result in parasitic drag [3]. The limiting factors when designing a system to control flow separation include energy consumption, weight, volume, complexity and cost [2].

Some popular passive flow control methods include sub-boundary layer vortex generators which produce stream-wise vortexes in the boundary layer that draw high-momentum fluid closer to the wall. They were introduced in the 1940s and have been utilised ever since to reduce flow separation in a wide variety of flows [4]. A lot of research has been focused on active flow control methods. Michelis et al. [5] investigated the response of a laminar separation bubble to impulse forcing caused by a dielectric barrier discharge plasma actuator. They found evidence linking incoming disturbances with the laminar separation bubble shear layer breakdown. Sang Hoon Kim and Chomgam Kim [6] investigated the aerodynamic characteristics of a NACA 23012 airfoil with synthetic jets. They found that the maximum lift was obtained when the separation point coincides with the synthetic jet location and the non-dimensional frequency is about 1. They also observed that the separation control effect was proportional to the peak velocity of the synthetic jet. Similary, using sweeping jet actuators on a NACA 0015 airfoil, LaTunia Pack Melton [7] found that a high momentum coefficient of the sweeping jet actuator was required for separation control when located downstream of the separation. Zong et al. [8] used an array of 26 plasma synthetic jet actuators flush-mounted on a NACA-0015 airfoil to control leading-edge separation at a Reynolds number of about $1.7 \times 10^5$. They found that the stall angle was increased by $22^o$, and the peak lift coefficient was increased by 21%. They also found that the

separation control was dependent on the relative location between the actuators and separation. This leads us to believe that some of the main factors affecting the effectiveness of active flow control are the location of the actuator relative to separation and the speed of the actuator.

This study investigates the use of a high-frequency translational piezoelectic stack actuator to control flow separation. Piezoelectric materials produce electricity when a force is applied to them. Interestingly enough, the reverse is also true; when electricity is passed through a piezoelectric material it produces a force as well as displacement by expanding or contracting. The latter characteristic is the basis for piezoelectric actuators. Multiple piezeolectric materials are placed on each other in several layers to create a piezoelectric stack actuator. When a voltage is applied to this piezoelectric stack actuator, an amplified displacement that's directly proportional to the voltage applied is generated; the amplified displacement is usually between 0.1 % and 0.15 % of the actuator length. The driving voltage of a piezoelectric stack actuator is directly proportional to the thickness of the layers; piezoelectric stack actuators can therefore be classified as low voltage and high voltage actuators.

Piezoelectric stack actuators have many useful applications. Yeom et al. [9] investigated the effects of piezoelectric translational agitator with an oval loop shell amplifier on improving the channel flow heat transfer. They discovered a 55% enhancement in convection heat transfer coefficient. This study, explores a new approach to flow control. The objective of this experiment is to observe the effect of the high-frequency translational piezoelectric actuators' oscillations amplified by an oval shell structure on delaying flow separation.

# Chapter 1

# Experiment Details

## 1.1 Oval Loop

The piezoelectric stack actuator typically generates small translational displacements. Therefore, the oval loop shell structure with dimensions as seen in Figure 1.1 was used to amplify the piezoelectric stack's small translational displacement using the resonance energy of the structure [10].

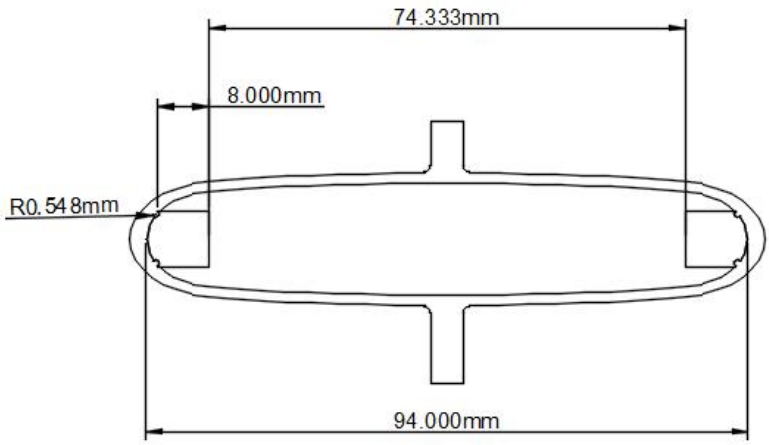


Figure 1.1: 2D Model of Oval Loop with Dimensions

There were two actuators embedded in the airfoil, therefore two oval loop structures were fabricated using steel. Each oval loop had a hole centered at the bottom extremity of the front face as well as two smaller holes equidistant from the center of the top extremity of the front face in order to attach the portion of the top of the airfoil it would oscillate. Figure 1.2 below shows the final design of the oval loop structures that were then fabricated. The actuators operated at a frequency of 565 Hz.

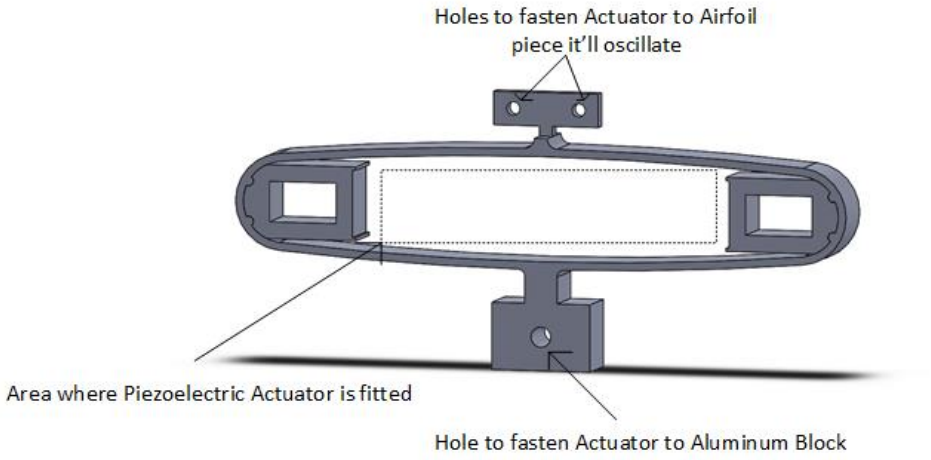


Figure 1.2: Oval Loop 3D CAD Model Showing Holes For Fasteners

The working principle behind the oval loop structure is that the piezoelectric stack actuator is fitted within the oval loop. The piezoelectric stack actuator then generates horizontal displacements and the oval loop amplifies this movement and converts it into vertical displacement. There are two resonance modes of the piezoelectric actuator within a 2 kHz frequency range that can provide amplified translational motion. At the first frequency mode, the bottom of the oval loop is excited thereby causing the entire oval loop body to oscillate vertically. However, in the second resonance mode, only the upper beam of the shell is excited and oscillated vertically [10].

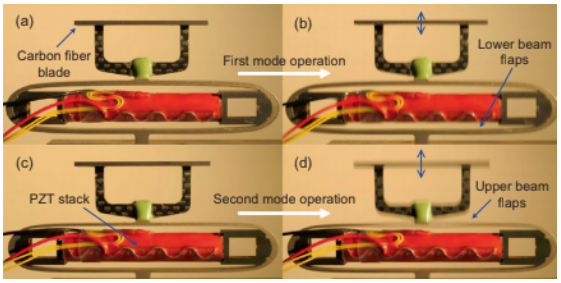


Figure 1.3: Oscillation of Actuator at First and Second Resonance Modes

## 1.2 Airfoil

The airfoil used in this study was the Eppler 862 seen in Figure 1.4. A symmetrical airfoil chosen to be able to fit in the wind tunnel as well as have enough space to contain the piezoelectric actuators used in the study.

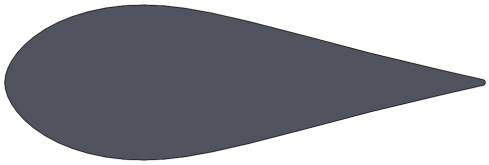

Figure 1.4: Eppler 862 2D CAD Model

The material chosen for the airfoil was PLA plastic. It was fabricated using a 3D printer with the specifications in Table 1.1. The actuators were to be embedded within the airfoil with the help of fasteners.

Table 1.1: Airfoil Dimensions

| **Property** | **Value** |
|---|---|
| Chord Length (cm) | 30.48 |
| Camber (cm) | 30.48 |
| Maximum Thickness (cm) | 4.94 |

The airfoil design was adjusted to accommodate the oval loop structure. The new design also made allowances for the actuator to be able to oscillate a part of the top of the airfoil which it was attached to.

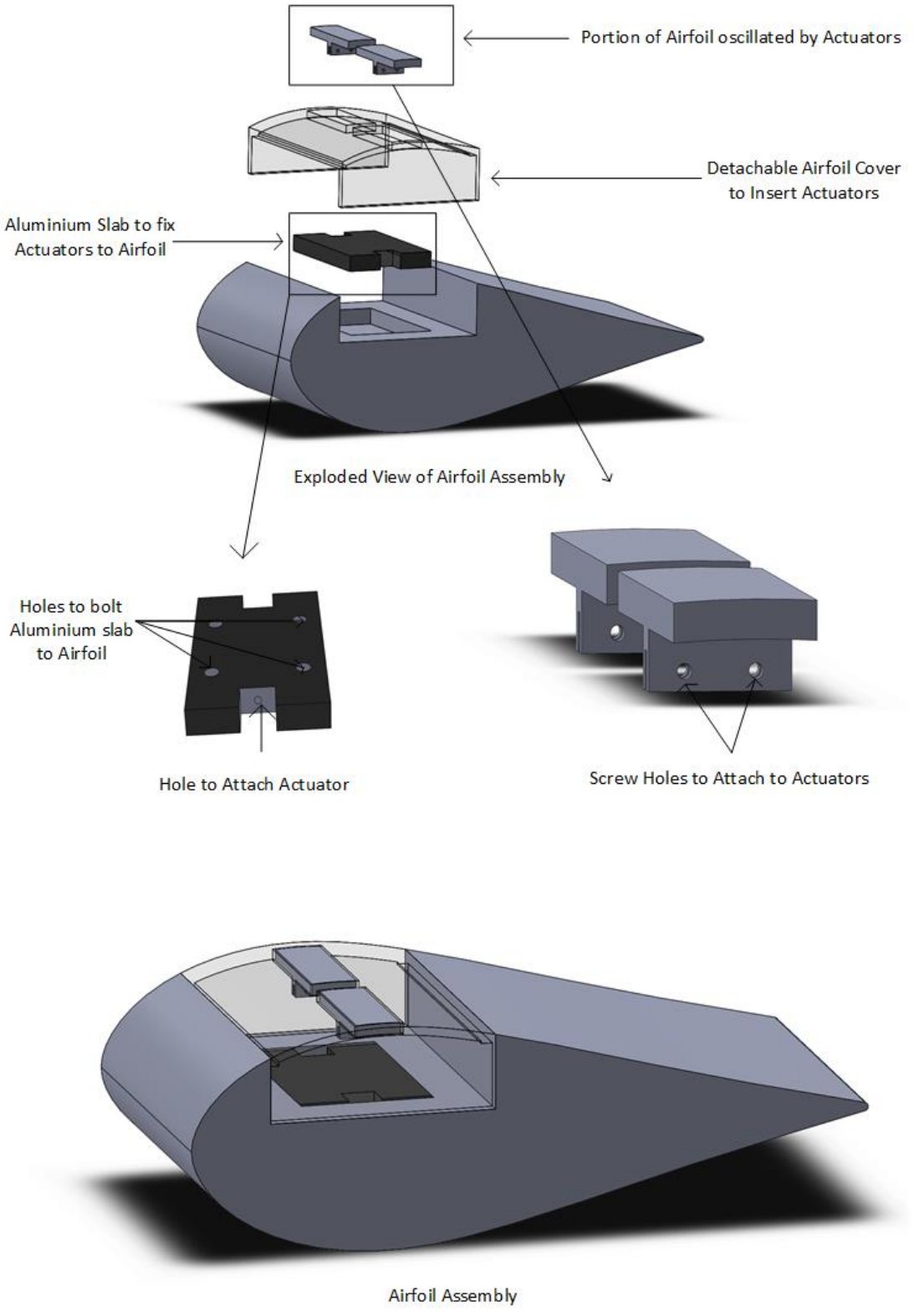


Figure 1.5: 3D Views of Airfoil CAD Model

## 1.3 Procedure

The experiments were conducted in the Pitsco X-Stream wind tunnel with a 48.26 cm × 29.21 cm × 29.21 cm testing chamber with speeds ranging from 0 m/s to about 18 m/s. Two holes were added to the airfoil along the chord line, a 5mm hole 50 mm from the leading edge and a 12.7 mm diameter hole 233.96 mm from the trailing edge, in order to properly fix the airfoil in the wind tunnel. The airfoil-actuator setup was placed in the wind tunnel and a device was used to set the angle of attack between $0^o$ and $28^o$ in increments of $2^o$. The freestream velocity was measured with a digital anemometer while the actuator displacement was measured with a Laser Doppler Vibrometer (LDV)

To visualise the flow in the wind tunnel, an Entour Ice fog generator was used to inject dry ice fog streams into the wind tunnel. A continuous laser was pointed parallel to the chord line and a Nikon 52 camera was observing from a position perpendicular to the chord line. The camera was used to take 5 sequential photos every 10 microseconds. Figure 1.6 shows the lab setup for the experiments.

The first step of the experiment was to confirm flow separation which was found to occur at a minimum angle of attack of about $6^o$ in low wind speeds. The parameters that were varied in this study were the actuator displacement, the angle of attack as well as the wind speed. Figure 1.7 shows a more detailed model of the experimental setup.

First of all, the actuator displacement was set to 0.0243 mm, 0.0463 mm, 0.0589 mm, 0.0821 mm and 0.1218 mm at wind tunnel wind speed of 4.3 m/s and at an angle of attack of $14^o$ to observe the effect of the actuator displacement on delaying flow separation. To observe the effectiveness of the actuators in separating flow at

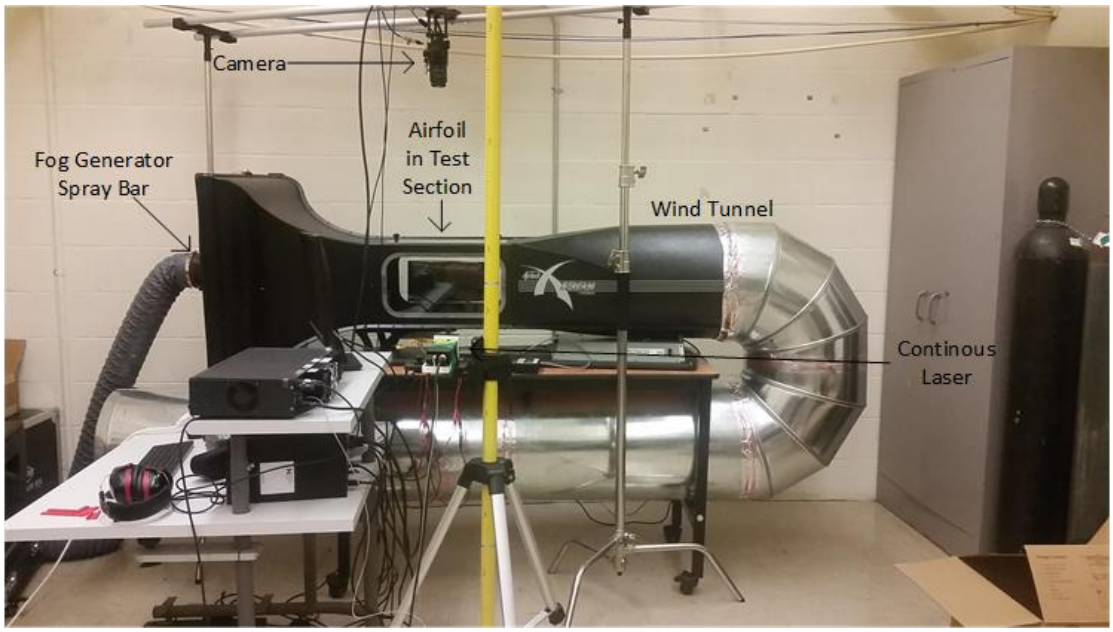


Figure 1.6: Experimental Setup

different wind speeds, the airfoil was inclined to an angle of attack of $14^o$ and data was taken for speeds of 4 m/s, 8 m/s and 12.71 m/s with an actuator displacement of 0.1139 mm. Finally, to observe the effectiveness of the actuator in separating flow at different angles of attack, wind speed was set to 4.3 m/s and the data was taken for angles of attack of $0^o$, $6^o$, $12^o$, $18^o$, $24^o$ with actuator displacement of 0.1139 mm.

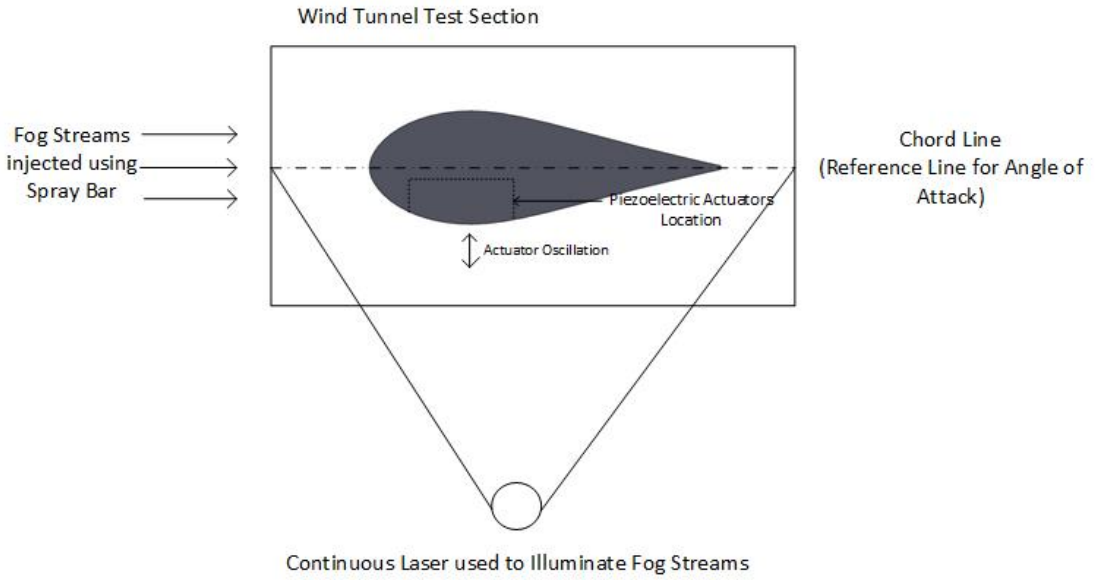


Figure 1.7: Model of Experimental Setup from the Camera's perspective

# Chapter 2

# Results and Analysis

Each of the settings for the actuator displacement, wind speed and angle of attack were varied one by one while keeping the other settings constant in order to evaluate it's effect on delaying flow separation. Table 2.1 shows the various voltage amplitudes the actuator was set to oscillate using the Koolertron Wave Amplifier and their equivalent displacements. The wind tunnel velocity was set to 4.3 m/s at an angle of a attack of $14^o$ for these experiments. The wave amplifier amplified the input wave by a magnitude of 40; the amplified values are listed in the Table 2.1. The Displacement values where measured using a laser doppler velocimetry (LDV) data acquisition system.

Table 2.1: Actuator Displacements Tested and Respective Voltages

| **Voltage (V)** | **Displacement (mm)** |
|---|---|
| 0 - 25 | 0.0243 |
| 0 - 50 | 0.0463 |
| 0 - 75 | 0.0589 |
| 0 - 100 | 0.0821 |
| 0 - 150 | 0.1218 |

The images in Figure 2.1 show the effect of the different displacements of the actuator on suppressing flow separation. The images on the left show the airflow around the airfoil when the actuator was not yet turned on and thus the flow developed naturally whereas the images on the right show the flow around the airfoil after the actuator had been turned. It is seen in Figure 2.1 that the actuator noticeably suppressed the flow separation even at a small displacement of 0.0243 mm and when the displacement reached 0.0589 mm, the actuator completely prevented flow separation from occurring.

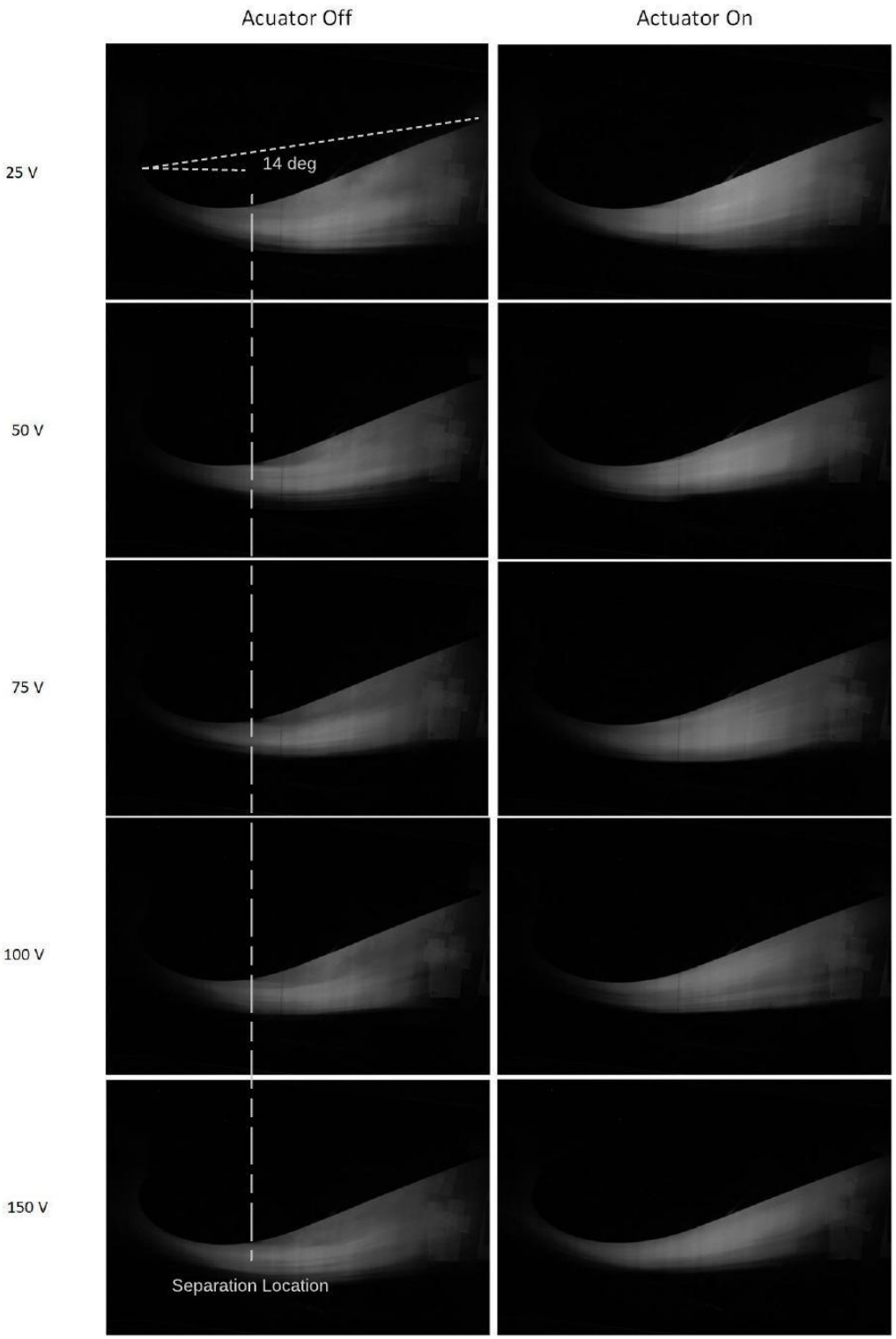


Figure 2.1: Effect of Actuator Displacement on Flow Separation

Next, the free stream velocity was varied while the actuator displacement was set to a displacement of 0.1139 mm at an angle of attack of $14^o$. Table 2.2 shows the various wind speeds that the wind tunnel was set to and their equivalent Reynold's numbers. It is seen that all the free stream velocities had Reynold's numbers less than $5 \times 10^5$ implying that all the experiments were conducted under laminar flow.

Table 2.2: Wind Speeds Tested and Respective Reynold's number

| **Velocity (m/s)** | **Reynold's Number** |
|---|---|
| 4.3 | $8.87 \times 10^4$ |
| 8 | $1.65 \times 10^5$ |
| 12.71 | $2.62 \times 10^5$ |

The images in Figure 2.2 show the effect of the different free stream velocities on the actuator's ability to suppress flow separation. The images on the left show the airflow around the airfoil while the actuator was still switched off and the images on the right show the flow around the airfoil after the actuator had been turned. It is seen in Figure 2.2 that the actuator completely prevented flow separation from occurring at a wind speed of 4.3 m/s but as the flow increased from 8 m/s upwards, flow separation began to occur again; although still noticeably suppressed.

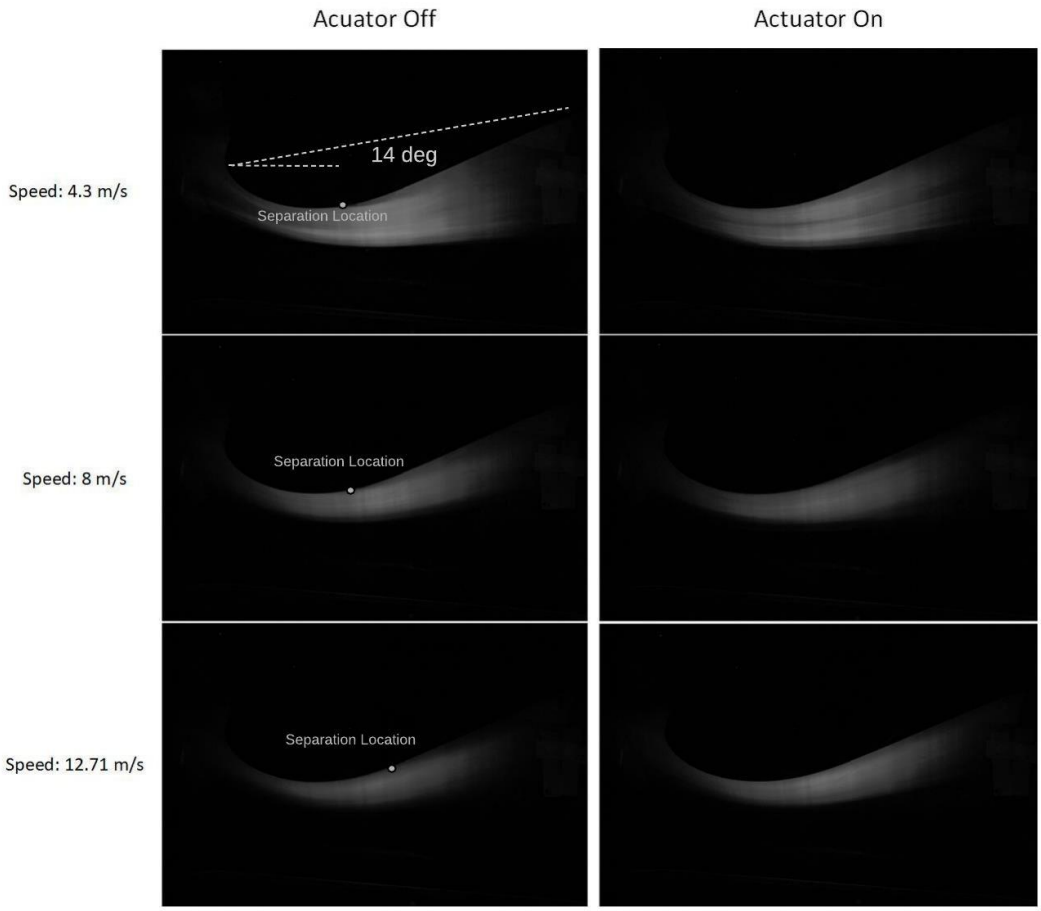


Figure 2.2: Free Stream Velocity Effect on Flow Separation

Finally, the angles of attack was varied at a wind tunnel wind speed of 4.3 m/s and actuator displacement of 0.1139 mm. The images in Figure 2.3 show the effect of the different angles of attack on the actuator's ability to suppress flow separation. The images on the left and right show the airflow around the airfoil before and after the actuator had been turned on respectively. It is seen in Figure 2.3 that the actuator completely prevented flow separation from occurring until an angle of attack of about $24^o$ which is about $18^o$ higher than it naturally occurs without the effect of the actuators. At the angle of attack of $24^o$, the flow separation was still suppressed.

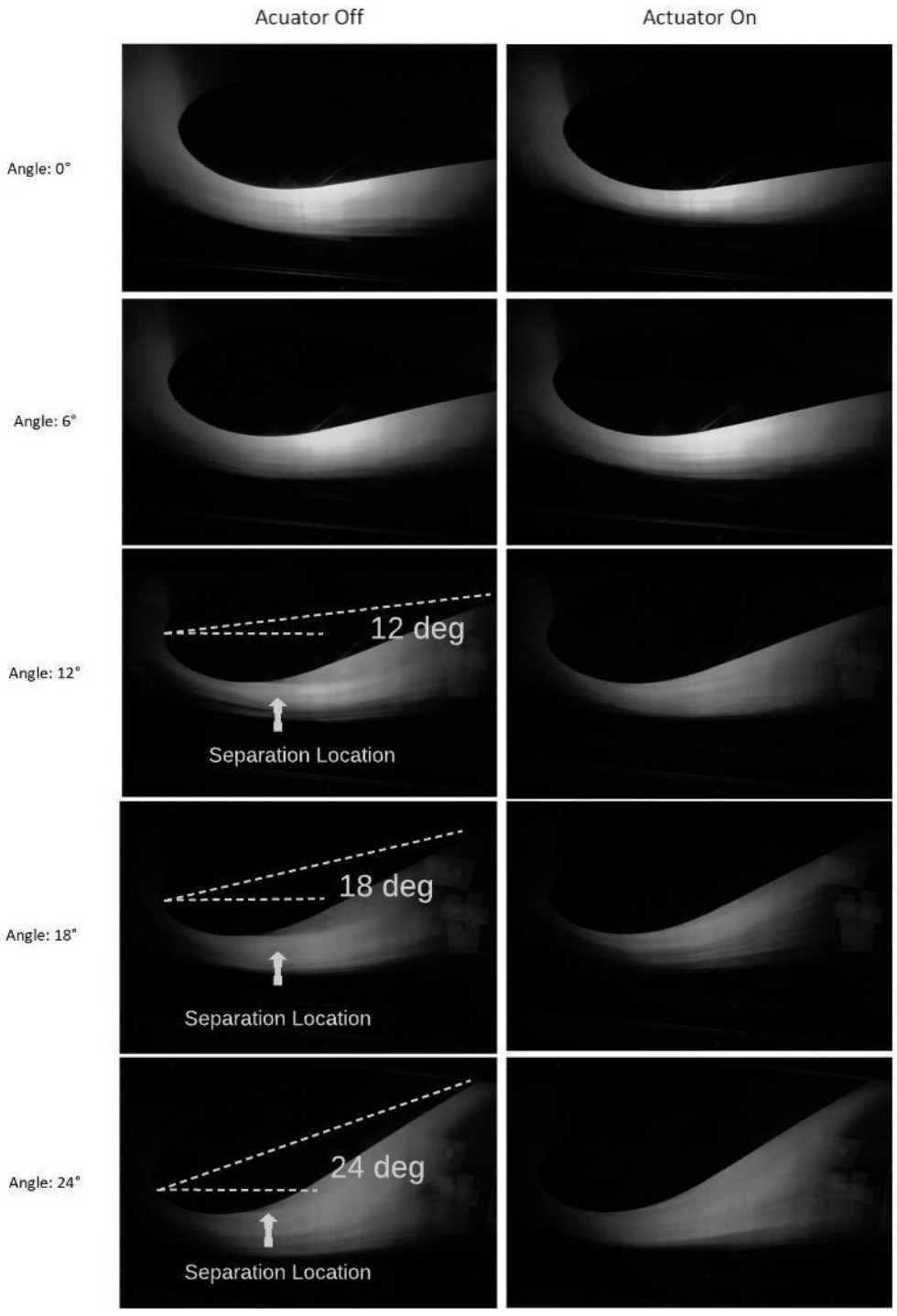


Figure 2.3: Angle of Attack Effect on Flow Separation

# Chapter 3

# Conclusion

This study aimed to delay flow separation on an airfoil by embedding two high-frequency translational piezoelectric actuators along the suction surface of the airfoil. This study investigated the extent to which the piezoelectric actuator displaces the flow separation downstream or prevents it altogether utilizing a fog-based flow visualization experiment on an Eppler 862 airfoil model placed in a low-speed wind tunnel. Sequential pictures of the airflow surrounding the airfoil were taken every 5 microseconds so as to observe the flow separation before and after turning on the high-frequency translational surface actuation. The effects of the actuation on the flow separation were observed at different surface displacements ranging up to 0.12 mm at a 565 Hz operating frequency, angles of attack ranging up to $24^o$, and wind tunnel free stream velocities increased up to 12.7 m/s.

Throughout the course of this study it was consistently seen that the actuators noticeably suppressed the flow separation. The flow separation was suppressed even at a small displacement of 0.0243 mm and was completely prevented when the displacement reached 0.0589 mm. For the wind speed, the actuators pre-

vented flow separation up until the wind speed reached 8 m/s at which point it continued to suppress it. Finally, the actuator completely prevented flow separation from occurring until an angle of attack of about $24^o$; about $18^o$ higher than it naturally occurs at which point it continued to suppress it. In summary, the high-frequency translational surface actuation was confirmed to have the effect of delaying or suppressing the flow separation over the airfoil depending on the parameters changed.

# Chapter 4

# Future Work

A recommendation for future work on this study would to use particle image velocimetry (PIV) to determine a more quantitative evaluation of the effect of the piezoelectric actuator on delaying flow separation. More data could also be collected in order to see if flow control equations can be derived. PIV involves injecting the fluid with with tracer particles which follow the flow. The fluid is then illuminated so that the tracer particles are visible. The motion of the tracer particles could then be used to calculate the velocity field of the flow being studied.

It is also worth considering the effect of the frequency of the translational surface on delaying flow separation. In this study, the frequency of the actuators was kept constant through out because the oval loop structure used in the experiments relied on resonance. Therefore in order to vary the frequency, more oval loop structures of varying natural frequencies would need to be fabricated. It is also worth varying the location of the actuators in the airfoil, the area of the translational surface and the number of actuators being used.

# Bibliography

[1] J. Flatt, "The history of boundary layer control research in the united states of america," *Boundary Layer and Flow Control*, vol. 1, pp. 122–143, 1961.

[2] M. Gad-el Hak and D. Bushnell, "Separation control: Review," *Journal of Fluids Engineering*, vol. 113, pp. 5–30, 1991.

[3] L. Cattafesta III and M. Sheplak, "Actuators for active flow control," *Annual Review of Fluid Mechanics*, vol. 43, pp. 247–272, 2011.

[4] B. Greene, N. T. Clemens, P. Magari, and D. Micka, "Control of mean separation in shock boundary layer interaction using pulsed plasma jets," *Shock waves*, vol. 25, no. 5, pp. 495–505, 2015.

[5] T. Michelis, S. Yarusevych, and M. Kotsonis, "Response of a laminar separation bubble to impulsive forcing," *Journal of Fluid Mechanics*, vol. 820, pp. 633–666, 2017.

[6] S. H. Kim and C. Kim, "Separation control on naca 2301 using synthetic jet," *Aerospace Science and Technology*, vol. 13, pp. 172–182, 2009.

[7] P. Melton and L. G, "Active flow separation control on a naca 0015 wing using fluidic actuators," in *7th AIAA flow control conference*, p. 2364, 2014.

[8] H. Zong, T. van Pelt, and M. Kotsonis, "Airfoil flow separation control with plasma synthetic jets at moderate reynolds number," *Experiments in Fluids*, vol. 59, no. 11, p. 169, 2018.

[9] T. Yeom, T. W. Simon, M. North, and T. Cui, "High-frequency translational agitation with micro pin-fin surfaces for enhancing heat transfer of forced convection," *International Journal of Heat and Mass Transfer*, vol. 94, pp. 354–365, 2016.

[10] T. Yeom, T. W. Simon, L. Huang, M. T. North, and T. Cui, "Piezoelectric translational agitation for enhancing forced-convection channel-flow heat transfer," *International journal of heat and mass transfer*, vol. 55, no. 25-26, pp. 7398–7409, 2012.